ANNALS OF THE UNIVERSITY OF ORADEA
FASCICLE OF TEXTILES, LEATHERWORK

PREDICTION OF ANTHROPOMETRIC INDICATORS DURING PREGNANCY THROUGH RADIUS-VECTOR ANALYSIS OF THE HUMAN BODY

GOSPODINOVA Mariya[1], KRASTEV Krasimir[2]

[1,2] Trakia University, Faculty of Technics and technologies, 38 Graf Ignatiev str., 8602, Yambol, Bulgaria

Corresponding author: GOSPODINOVA Mariya, e-mail: mimoza.1982h@gmail.com

Abstract: *The insufficient adaptation of clothing and medical devices to the dynamic morphological changes of the human body during pregnancy poses significant challenges to contemporary anthropometry, ergonomic design, and personalized product development. In this study, digital images of 81 silhouettes of pregnant women's bodies were analyzed to explore the potential of radius-vector–based geometric descriptions for predicting key anthropometric indicators. From each silhouette, normalized radius-vector functions were extracted, and five geometric indices (FI1–FI5) were calculated, characterizing symmetry, convexity, proportionality, deviation from a reference silhouette, and local curvature. These indices were evaluated for their informativeness using FSRNCA, RReliefF, and SFCPP feature-selection methods. Regression models were subsequently developed to predict body mass, month of pregnancy, waist circumference, and uterine height. The results demonstrate that radius-vector functions provide mathematical representation of the pregnant body silhouette, enabling the extraction of anthropometric characteristics. FI5 (local curvature) and FI2 (convexity) emerged as the most informative indices across multiple prediction tasks. The model for estimating the month of pregnancy achieved the highest predictive accuracy (R^2 = 0.68), followed by the model for uterine height (R^2 = 0.59). Residual analyses confirmed good model fit for these two characteristics, while models for body mass and waist circumference showed moderate predictive capability. The findings highlight the potential of silhouette-based geometric analysis as an accessible, non-invasive, and cost-effective approach for monitoring morphological changes during pregnancy. This methodology can support the development of adaptive clothing, personalized medical devices, and digital simulations for obstetric and ergonomic applications.*

Keywords: *radius-vector function, anthropometrics, pregnancy, regression model, adaptive design*

1. INTRODUCTION

The development of functional and aesthetic garments for pregnant women requires a detailed analysis related to the changes in the body during pregnancy. Traditional methods of clothing design often do not take into account the individual characteristics of body morphology, which leads to discomfort, limited mobility, and compromise with the woman's vision. Geometric analysis of the silhouette characteristics of the pregnant woman's body provides opportunities for personalized and adaptive clothing design.

Modern methods for determining the dimensions of the human body vary significantly in terms of accuracy, accessibility, and applicability. Three more commonly used methods for obtaining the body dimensions of pregnant women can be summarized – classic measurements with a sewing tape, image acquisition and processing, and the application of 3D scanning.

Traditional anthropometric methods, based on manual measurements [1] using instruments such as tape measures, anthropometers, and calipers, remain widely used due to their accessibility and standardization [2, 3]. They allow direct measurement of body dimensions and are well-established in clinical practice, garment design, and scientific research. The main limitations of this approach include

subjectivity, the possibility of human error, and the difficulty of self-measurement. Furthermore, the method does not provide spatial information about body geometry and volume.
Table 1 presents a comparative analysis of methods for determining anthropometric dimensions.

Photo-based techniques [4] offer a sufficiently high degree of convenience and the possibility of remote data collection, making them suitable for large population studies and application in online platforms. They require minimal equipment and allow the extraction of multiple anthropometric parameters from ordinary digital images. However, the accuracy of these methods depends on the quality of visualization, lighting, and body position, which limits their reliability for precise measurements.

The application of 3D scanners is a modern approach to anthropometric measurements, which provides sufficiently high accuracy, speed, and the ability to create detailed 3D models of the human body [5, 6]. They allow automated extraction of a sufficiently large number of anthropometric parameters and are suitable for designing personalized clothing, including for specific groups such as pregnant women. Despite its advantages, this method requires equipment with a higher cost compared to photographic images and classical measurement methods and specialized infrastructure, which limits its accessibility for wider use.

***Table 1**: Comparative analysis of methods for determining anthropometric dimensions*

Method	Accuracy	Applicability in pregnancy	Accessibility	Source
Classical anthropometric measurements	Average – depends on experience of the measurer	Limited – difficult to track dynamic changes	High – cheap measuring tools	[7]
Photo-based methods	Low to medium – depends on image quality	Partially applicable – difficult to capture volumetric changes	Very high – only camera and app	[8]
3D scanning	High – captures volumetric and spatial changes	Excellent – tracks non-linear changes throughout gestation	Low – expensive equipment and software	[9]

In the reviewed available scientific literature sources, the focus is mainly on linear and volumetric measurements applicable to the design of clothing for pregnant women, but there is a lack of in-depth analysis of the morphology and its dynamics through mathematical descriptions. Mathematical functions that describe the silhouettes of the body during the different stages of pregnancy in polar or parametric form have not been used, nor have geometric indices derived from them been defined – such as curvature, symmetry or local deformations. Such type of analyses will provide sufficient precision in the creation of adaptive structures and personalized clothing, especially in the dynamic transformation of the female body during the gestation period.

The photo-based method for determining human body dimensions offers a combination of accessibility, speed, and sufficient accuracy, which makes it particularly suitable for studies with large samples and dynamic changes in the human body, such as those that occur during pregnancy. Unlike classical measurements, which are laborious and subjective, and 3D scanning, which requires expensive equipment and a specialized environment, photo-based measurements allow data collection with minimal resources and without physical contact with the photographed object. According to García Flores et al. [10], the photo-based approach shows a lower average error and a shorter measurement time compared to 3D scanning, making it more effective in a practical environment. This feature makes it a suitable tool for analyzing the body silhouette of pregnant women and for creating adaptive clothing based on real and current characteristics of the human body.

The aim of this study is to propose a way to determine body changes using mathematical functions that describe the silhouettes of the pregnant woman's body. These descriptions of changes in the silhouette of the pregnant woman's body are suitable for creating adaptive, personalized clothing, building on existing approaches that do not take into account the dynamics and complexity of the female body silhouette during the gestational period.

2. MATERIAL AND METHODS

A total of 81 body silhouette images were used, representing changes in the body of women during pregnancy. The search for body silhouettes of pregnant women on the Internet was done using the keywords – "pregnancy period", "Pregnant woman silhouette", "Maternity silhouette", "Maternity 9 months". The body silhouettes are free to download and were used solely and exclusively for the purposes of this study. They were downloaded from the following Internet sources:

Source	Accessed on:
https://www.vecteezy.com	17.07.2025
https://www.123freevectors.com	11.07.2025
https://www.freepik.com	28.06.2025
https://www.freevector.com	25.06.2025
https://www.instagram.com	12.06.2025
https://de.pinterest.com	12.06.2025

After being downloaded, the silhouettes of the pregnant women's bodies were separated into separate objects from the original image. They were vectorized in Inkscape ver. 1.0.1 (https://inkscape.org, accessed 12.07.2025). After this procedure, the separate silhouettes of the pregnant women's bodies were exported to *.png file format for further processing. In Appendix A, Figure A1, the used silhouettes of the pregnant women's bodies are presented.

The description of the contours of the pregnant women's body silhouettes was made using a radius-vector function [11, 12]. In this work, the calculation of the radius-vector functions starts from the top point of the object. The obtained values are normalized to the height of the pregnant woman's body silhouette. The following notations are used when presenting the mathematical formulas:

$$C = (x_c, y_c) \in R^2 \quad \text{Center of gravity of the object} \quad \textbf{(1)}$$

$$\{P_i = (x_i, y_i)\}_{i=1}^{N} \quad \text{The points on the object's contour, which are N in number} \quad \textbf{(2)}$$

$$\theta \in [0, 2\pi] \quad \text{Polar angle relative to horizontal axis} \quad \textbf{(3)}$$

A total of 360 measurements (k) are made from the center of gravity to points on the object's contour, in the interval [0, 2π]:

$$\theta_k = \frac{2\pi(k-1)}{360}, \quad k = 1, 2, \dots, 360 \quad \textbf{(4)}$$

In order to standardize the starting point, each radius-vector function starts from the top point of the body silhouette, defined by:

$$j^* = \arg \min_{i \in \{1,\dots,N\}} y_i \quad \textbf{(5)}$$

The loop is then rearranged so that P_{j*} becomes the starting point and the others follow cyclically:

$$B' = \{P_{j*}, P_{j*+1}, \dots, P_N, P_1, \dots, P_{j*-1}\}, \qquad P_j = (x_j, y_j), \qquad j = 1, \dots, N \quad \textbf{(6)}$$

For each θ_k, the nearest point P_j is chosen whose angle with respect to the center of gravity C is closest to θ_k:

$$\mathrm{j} = \arg\min_j \left| atan2(y_j - y_c, x_j - x_c) - \theta_k \right| \quad \textbf{(7)}$$

The distance from the center to the selected point P_j determines the value of the radius at the corresponding angle:

$$r(\theta_k) = \sqrt{(x_j - x_c)^2 + (y_j - y_c)^2} \quad \textbf{(8)}$$

The radius-vector function is normalized to the height of the pregnant woman's body (H):

$$r_n(\theta_k) = \frac{r(\theta_k)}{H}, \quad H = \max_i y_i - \min_i y_i \quad \textbf{(9)}$$

The resulting generalized equation, by which the normalized radius-vector function is calculated, has the form:

$$r_n(\theta_k) = \frac{1}{H}\min_j \left\{ \sqrt{(x_j - x_c)^2 + (y_j - y_c)^2} \middle| \theta_j = atan2(y_j - y_c, x_j - x_c) \approx \theta_k \right\}, \quad \theta_k = \frac{2\pi(k-1)}{360} \quad \textbf{(10)}$$

Using the obtained radius-vector functions characterizing the silhouettes of the body of pregnant women, indices reflecting changes in the body were calculated. These indices were summarized based on available literature sources [13, 14, 15, 16, 17].

FI1 is an index of symmetry. It assesses the degree of symmetry of the silhouette of the pregnant woman's body relative to a vertical axis passing through the center of the body. During pregnancy, especially in advanced stages, asymmetries may occur, for example, due to posture, pressure from the fetus or unilateral displacement. FI2 is an index of convexity. It reflects the relative convexity of the abdomen in the anterior part of the silhouette of the pregnant woman's body, relative to the average body size. The index can be used as an indicator of pregnancy progress, as its value increases with advancing gestation. The index is sensitive to changes in the anterior projection of the abdominal region. FI3 is a body silhouette index that describes the overall proportion between the maximum radial length of the body (the most prominent point) and its average radius. The index indicates the extent to which the body silhouette changes from a uniform (circular) to a more irregular, convex structure characteristic of advanced pregnancy. FI4 is an index measuring the difference between the current body silhouette and a reference (initial) silhouette of the pregnant woman's body. It is used to quantify dynamic changes in the body silhouette between individual gestational weeks. The index is suitable for longitudinal monitoring of morphological development during pregnancy.

FI5 assesses the variation in the local curvature of the pregnant woman's body silhouette along its entire circumference. High values of this index reflect irregularities and abrupt changes in the pregnant woman's body silhouette such as sharp contours, local protrusions or uneven expansion. This index is sensitive to structural changes in the body, including changes in the breasts, abdomen and pelvis. The body silhouette indices of pregnant women have the following form:

$$FI1 = \frac{1}{\pi}\int_0^{\pi} \frac{|R(\theta) - R(\pi - \theta)|}{\bar{R}} d\theta \quad \textbf{(11)}$$

$$FI2 = \frac{R(\theta_{max})}{\bar{R}} \quad \textbf{(12)}$$

$$FI3 = \frac{R_{max}}{\bar{R}} \quad \textbf{(13)}$$

$$FI4 = \frac{1}{2\pi}\int_0^{2\pi} \frac{|R_t(\theta) - R_0(\theta)|}{\bar{R}_0} d\theta \quad \textbf{(14)}$$

$$FI5 = \sqrt{\frac{1}{2\pi}\int_0^{2\pi}(R'(\theta) - \bar{R}')^2 d\theta} \quad (15)$$

where R(θ) is a radius-vector function; $\bar{R}$ is the average value of R(θ); R_{max} is the largest radius, relative to the center of gravity of the object; the angle θ changes in the interval θε[0, 2π]; $R_t(\theta)$ is the current value of the radius; $R_0(\theta)$ is the initial radius; R'(θ) is the first derivative of the radius-vector function R(θ) with respect to the angle θ.

The informativeness of body silhouette indices in pregnant women was determined using the FSRNCA, RreliefF, and SFCPP selection methods. FSRNCA (Feature Selection for Classification and Regression by Neighboring Component Analysis). This method identifies the most appropriate body silhouette indices of expectant mothers, using their weights obtained in such a way as to minimize the prediction error [18]. RReliefF is used for feature selection in regression tasks. It evaluates the importance of features based on their ability to distinguish data that are close to each other [19]. This algorithm is suitable for assessing the significance of features for distance-based models. SFCPP (Feature Selection with Comparable Predictive Ability). A feature selection method in which the identification of those with similar predictive capabilities while reducing data redundancy [20]. Informative are those indices that have weight coefficients with a value above 0.6 [21].

Data on pregnant women's body mass, waist circumference and uterine height, measured during the implementation of previous scientific projects [22], were used. These data are presented in Table 2.

***Table 2**: Data from measurements of pregnant women*

Characteristic / Month	BW, kg	WC, cm	UH, cm
M1	55±5	75,44±5,17	15±3,08
M2	55±5	75,44±5,13	15±1,76
M3	55±5	75,44±5,17	15±3,08
M4	58±5	79,78±5,74	17,89±2,71
M5	60±5	84±6,06	21,22±2,28
M6	62±4	87,33±5,24	25±2,06
M7	65±4	91,11±5,3	27,22±1,48
M8	66±5	95,11±3,95	30,67±1,32
M9	68±5	98±3,04	33±1,12
BW-body weight; WC-waist circumference; UH-uterine height			

The ability to predict data from measurements of pregnant women was tested using a second-order polynomial regression model, which is more commonly used in practice [23]. The model describes the relationship between the independent and dependent variables and has the following form:

$$z = b_0 + b_1x + b_2y + b_3x^2 + b_4xy + b_5y^2 \quad (16)$$

where z is the dependent variable. The independent variables are x and y; the coefficients of the model are denoted as b.

The regression model was evaluated based on: Coefficient of determination (R^2); Values of the regression coefficients; Standard error (SE) of the regression coefficients; p-values of the coefficients and of the model; Value of the Fisher test (F) compared to the critical value Fcr. An analysis of the residuals of the regression model was performed.

The processing of the experimental data was carried out in the Matlab 2017b programming environment (The Mathworks Inc., Natick, MA, USA).

All statistical analyses were performed at a level of significance α=0,05.

3. RESULTS

The developed algorithm for determining a normalized radius-vector function along the contour of a pregnant woman's body silhouette is presented in Figure 1. The RGB image is converted to HSV color space and the saturation channel (S) is extracted to isolate the object (the silhouette of a pregnant woman's body) along a given saturation range. Then, a binary gradient mask is created, the object contours are found, and the center of gravity is calculated. The contour is rearranged so that it starts from the top point of the pregnant woman's body silhouette. In this way, each radius-vector function starts from the same point. For each point, an angle and radius are calculated relative to the center of gravity. Based on these values, a radius-vector function with 360 samples is built, which is normalized by the height of the figure and smoothed. Finally, the results are visualized graphically - both in the form of a function and by marking a contour, center, and starting point on the pregnant woman's body silhouette.

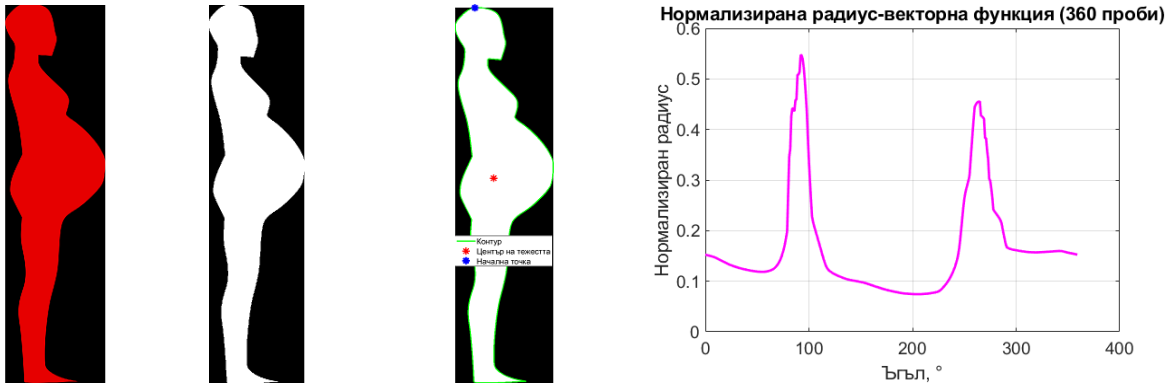

a) original RGB image | b) S(HSV) component of the image | c) object outline with characteristic points | d) normalized radius-vector function

***Fig. 1**: Algorithm for obtaining a normalized radius-vector function of a pregnant woman's body silhouette*

Figure 2 presents averaged normalized radius-vector functions for the stages of pregnancy (from M1 to M9). As pregnancy progresses (from M1 to M9), progressive changes in the radii are observed - most significantly around 75°, which reflects the abdominal area. There, the radii increase significantly, showing the typical increase in volume in the front of the body. This affects maternity clothes, which must follow these changes, ensuring comfort, freedom of movement and aesthetics.

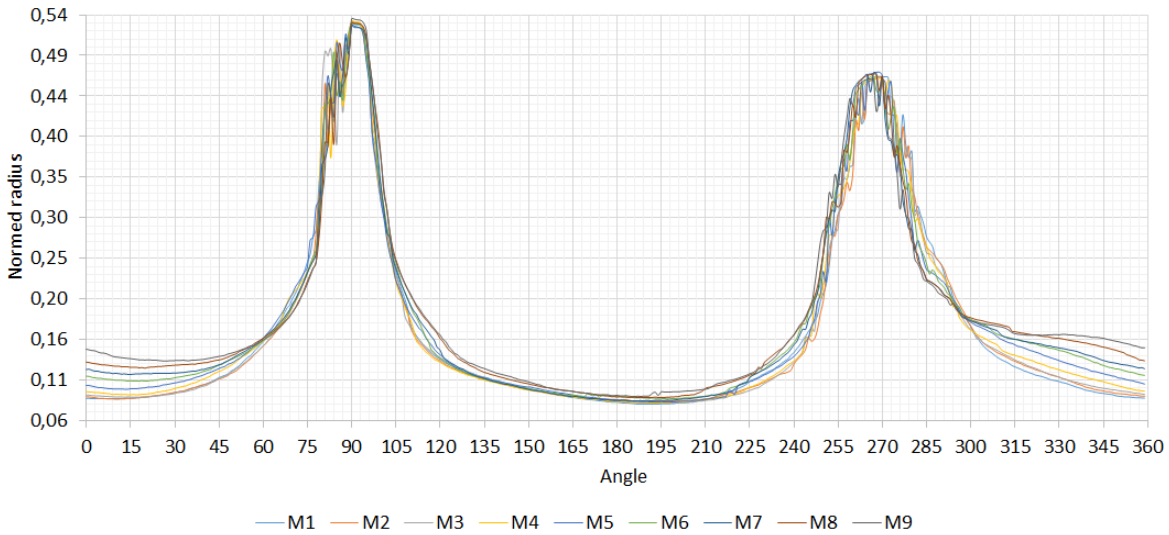

***Fig. 2**: Averaged normalized radius-vector functions representing stages of pregnancy in women*

Table 3 presents the calculated values of the body silhouette indices of women during pregnancy. Analysis of the results from the table shows a clear dynamics in the morphology of the body silhouette of pregnant women during the gestation period. FI1 (symmetry index) gradually increases from 0,19 to 0,29, which suggests a slight increase in asymmetry due to changes in posture and pressure from the fetus. FI2 (convexity index) has a tendency to increase from 1,11 to 1,63, reflecting the progressive enlargement of the abdominal area. FI3 (shape index) shows a tendency to decrease – from 3,36 to 3,02 – which indicates a transition from a more even to a more convex and uneven body silhouette, typical of advanced pregnancy. FI4 remains relatively constant (0,02), which is due to the use of a fixed reference body silhouette (in the first month of pregnancy), as well as the limited sensitivity of the index to monthly changes. FI5 (local curvature index) shows the most significant increase compared to the other indices – from 0 to 0,24 – which indicates increasing structural complexity and the appearance of local irregularities in the silhouette of the pregnant woman's body, especially in the abdomen, chest and pelvis.

***Table 3**: Values of body geometrical indices of pregnant women*

Index / Month	FI1	FI2	FI3	FI4	FI5
M1	0,19±0,07	1,11±0,24	3,36±0,66	0,02±0,01	0±0
M2	0,21±0,05	1,1±0,19	3,36±0,57	0,02±0,01	0,06±0,04
M3	0,23±0,05	1,13±0,2	3,33±0,6	0,02±0,01	0,08±0,03
M4	0,25±0,03	1,21±0,28	3,32±0,58	0,02±0,01	0,11±0,04
M5	0,25±0,05	1,26±0,22	3,24±0,56	0,02±0	0,13±0,04
M6	0,27±0,04	1,33±0,24	3,14±0,55	0,02±0	0,15±0,04
M7	0,28±0,07	1,45±0,25	3,15±0,47	0,02±0	0,17±0,06
M8	0,29±0,06	1,49±0,26	3,06±0,51	0,02±0	0,22±0,07
M9	0,28±0,06	1,63±0,28	3,02±0,46	0,02±0	0,24±0,09

Figure 3 shows the results of the selection of informative signs for predicting the month of pregnancy, human body mass, waist circumference and uterine height.

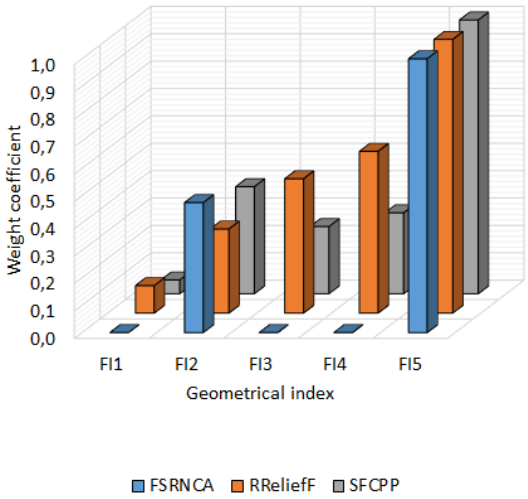

a) month of pregnancy (M)

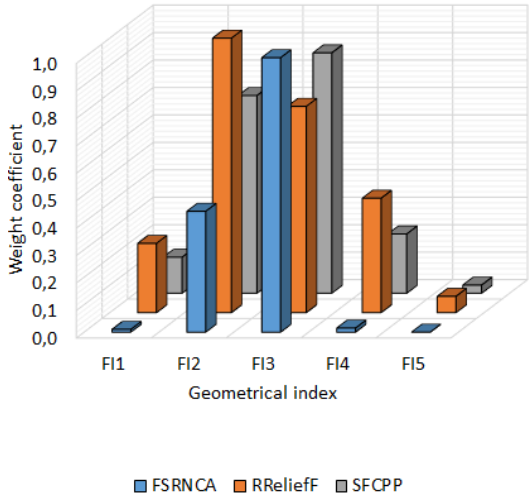

b) body weight (BW)

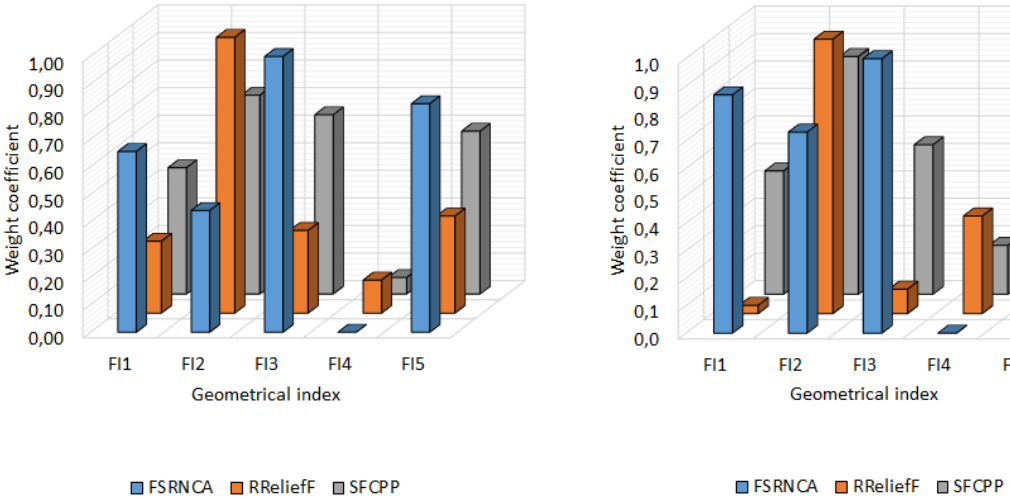

c) waist circumference (WC) d) uterine height (UH)

***Fig. 3**: Selection of informative features*

The appropriate pair of indices for predicting the month is FI5 and FI4. FI5 clearly meets the criterion of informativeness, since it has weighting coefficients above 0,6 by all methods and is appropriate for predicting several of the characteristics of the human body during pregnancy. For body mass (W), the most informative are the indices FI2 and FI3, which have high values by all methods (FI2 is 1,00 by RReliefF and 0,72 by SFCPP; FI3 is 1,00 by FSRNCA and 0,88 by SFCPP), which makes them a suitable pair for predicting body mass. For waist circumference (WC), the most relevant indices are FI3 and FI5, both of which have weighting coefficients above 0,6 by FSRNCA and SFCPP, and FI5 has the highest summary value among the other indices. Regarding uterine height (HM), the best predictors are FI2 and FI5, which show high significance by all methods (FI2 has a weighting coefficient of 0,73 by FSRNCA, 1,00 by RReliefF and 0,87 by SFCPP; FI5 is 0,83, 0,66 and 0,74 respectively).

Regression models were constructed to test the ability to predict month of pregnancy (M), body weight (BW), waist circumference (WC), and uterine height (UH) from geometric data obtained from body profile silhouettes of pregnant women. After removing the insignificant coefficients from the regression models with p>α, the models have the form:

$$M = 1{,}49 + 34{,}6FI5 - 165{,}1FI4^2 - 36{,}3FI5^2 \quad \textbf{(17)}$$

$$BW = 106{,}96 - 33{,}68FI3 + 3{,}95FI2^2 + 5{,}17FI3^2 \quad \textbf{(18)}$$

$$WC = 123{,}66 - 29{,}6FI3 + 4{,}38FI3^2 + 23{,}6FI3FI5 \quad \textbf{(19)}$$

$$UH = 12{,}1 + 48{,}44FI5 + 2{,}21FI2^2 \quad \textbf{(20)}$$

Table 4 presents the results of the regression model evaluation. The best predictive value among the analyzed models is shown by the one for M=f(FI4, FI5) with a coefficient of determination R^2=0,68, which means that 68% of the variation of the dependent variable is explained by the independent variables. This model also has the lowest standard error (SE=1,51), which further confirms its precision. The second most effective model is the model BM=f(FI2, FI5) with R^2=0,59 and a significantly high value of the F-criterion (F=54,94), exceeding the critical value Fcr=3,11. The models OT=f(FI3, FI5) and W=f(FI2, FI3) show lower values of R^2 – 0,43 and 0,26, respectively – which indicates their weaker explanatory power. However, all models are statistically significant, as the p values are below 0,00, confirming the presence of a significant relationship between the studied independent and dependent variables.

***Table 4**: Results of regression model estimation*

Model	R^2	F	Fcr	SE	p-value
M=f(FI4, FI5)	0,68	F(3, 77)=53,31	2,72	1,51	<0,00
BW=f(FI2, FI3)	0,26	F(3, 77)=8,23	2,72	5,89	<0,00
WC=f(FI3, FI5)	0,43	F(3, 77)=19,43	2,72	7,39	<0,00

UH=f(FI2, FI5)	0,59	F(2, 78)=54,94	3,11	4,59	<0,00
R^2-coefficient of determination; F-Fisher's test; Fcr-critical value of F; SE-standard error					

Figure 4 shows the obtained regression models in general. The presented models demonstrate diversity in the structure and degree of explanatory power in relation to the dependent variables. The shape of these surfaces varies - in models with higher values of the coefficient of determination R^2, such as M=f(FI4, FI5) and BM=f(FI2, FI5), a smoother and more clearly expressed surface is observed, which indicates a stable and predictable relationship between the variables. Conversely, the models W=f(FI2, FI3) and OT=f(FI3, FI5) show a more scattered and uneven regression shape, which corresponds to their lower explanatory power. However, all models are statistically significant, which is confirmed by the values of p<0,00. The model M=f(FI4, FI5) is most informative at medium to high values of FI4 and FI5, where the dependent variable M shows a stable and predictable change. Similarly, BM=f(FI2, FI5) is more informative at high values of FI5, which is reflected in the distinct shape of the regression surface.

Figure 5 shows normal probability plots of the residuals for the obtained regression models. The plots show slight deviations from the straight line, especially for the models W=f(FI2, FI3) and OT=f(FI3, FI5). These models exhibit more pronounced tails, which suggests the presence of extreme values and deviations from the normal distribution of the residuals. This is a sign of a weaker adaptation of the model to the real data. On the other hand, the models M=f(FI4, FI5) and BM=f(FI2, FI5) show a close location of the residuals to the straight line, which is an indicator of normality and more accurate regression estimates compared to the other two models considered.

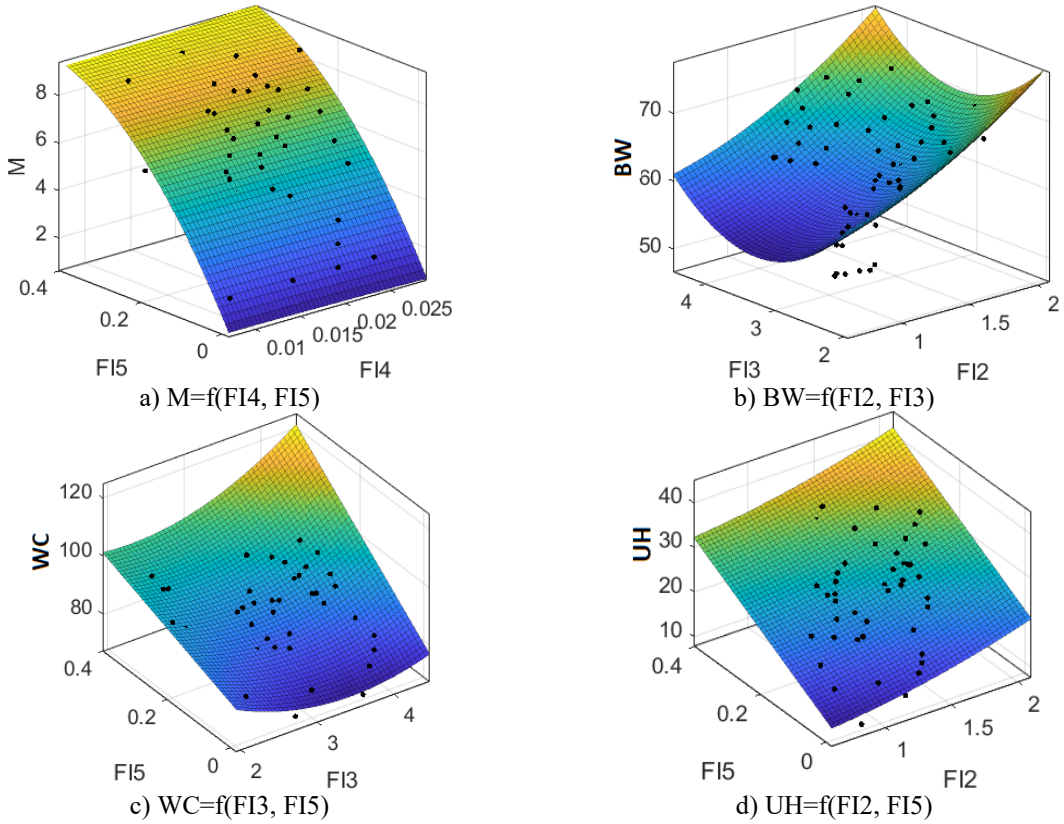

a) M=f(FI4, FI5) b) BW=f(FI2, FI3)

c) WC=f(FI3, FI5) d) UH=f(FI2, FI5)

***Fig. 4**: Regression models for predicting the body size of pregnant women – general view*

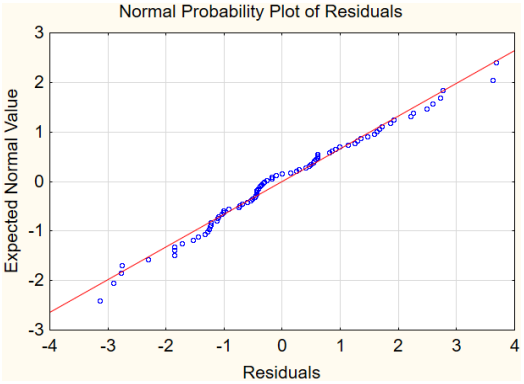

a) M=f(FI4, FI5)

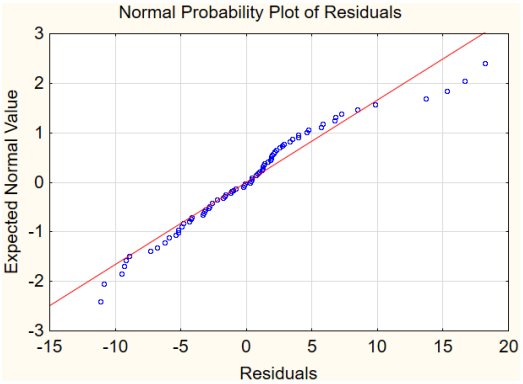

b) BW=f(FI2, FI3)

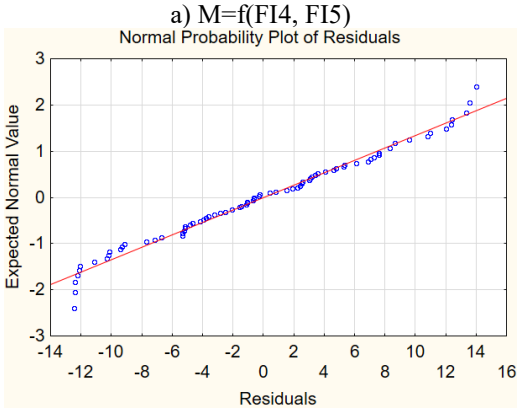

c) WC=f(FI3, FI5)

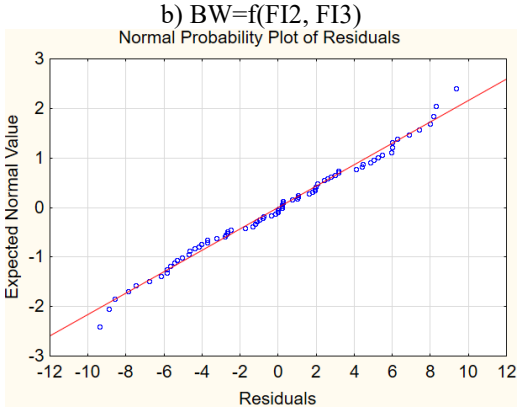

d) UH=f(FI2, FI5)

***Fig. 5**: Normal probability plots for the resulting regression models*

Figure 6 shows the distribution of the residuals for the obtained regression models. In the models M=f(FI4, FI5) and BM=f(FI2, FI5), the distribution of the residuals is closest to normal, which is evident from the symmetrical shape of the histograms and the good fit to the normal curve. This indicates that the models adapt to the data and that the assumption of normality of the errors is relatively fulfilled. In the models W=f(FI2, FI3) and OT=f(FI3, FI5), deviations from the normal distribution are observed - the residuals are more scattered and there is a presence of asymmetry, which is a sign of heteroscedasticity or the presence of unregistered factors that affect the accuracy of these regression models.

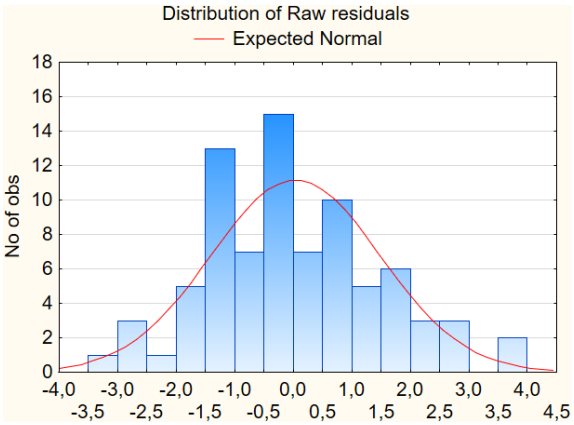

a) M=f(FI4, FI5)

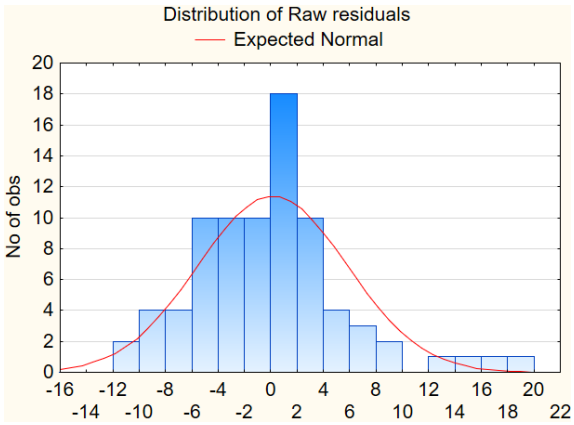

b) BW=f(FI2, FI3)

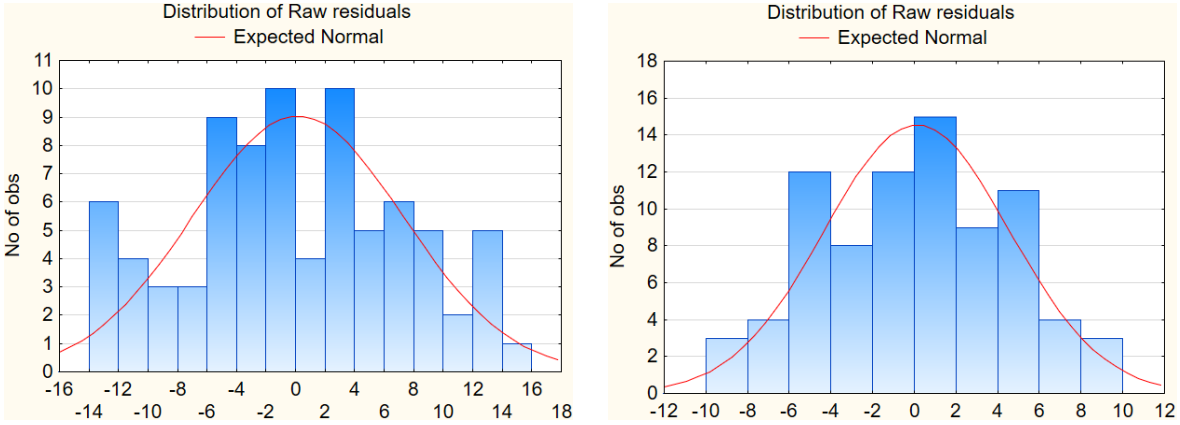

c) WC=f(FI3, FI5) d) UH=f(FI2, FI5)

***Fig. 6**: Distribution of residuals for the resulting regression models*

4. DISCUSSION

The results obtained in this study show that the FI1–FI5 indices are suitable for quantitative assessments of symmetry, convexity, and local deformations of the body silhouette, which builds on the traditional linear and volumetric measurements of pregnant women used in the available literature. Salzer et al. [24] point out that most existing tools for assessing the body silhouette of pregnant women focus on psycho-emotional aspects, but do not include geometric or mathematical descriptions of their body silhouette. This shortcoming is addressed in the present study. The regression models based on the indices proposed in this study show varying degrees of predictive power – the model M=f(FI4, FI5) with R^2=0,68 shows a sufficiently high accuracy, which complements the results of Bao et al. [25] that the use of complex regression structures (including hybrid models) significantly improves the predictive ability in human body measurements. On the other hand, the model W=f(FI2, FI3) with R^2=0,26 shows limited predictive ability, which complements the observations of Bicevskis et al. [26] that linear models often fail to capture nonlinear relationships between different characteristics of the human body. Residual analysis further confirms the reliability of the models for predicting month of gestation (M) and uterine height (BM), showing a normal distribution of errors, while the models for body mass (W) and body circumference (OT) have larger biases, which is typical of less well-adapted models. This complements the findings of Choutas et al. [27] that the accuracy of measuring human body dimensions and determining its silhouettes is important for applications such as virtual garment visualization and personalized designs, and that models that do not capture the real body silhouette lead to compromises in the final product and failure to meet customer requirements.

The results of this work can be useful in designing clothing for pregnant women by using radius-vector functions to model basic body proportions by month, which facilitates the creation of elastic adaptive or transformable clothing with the ability to predict changes in dimensions for future stages, supporting the production of clothing that "grows" with the body and detecting areas with the greatest changes, such as the abdomen and back, in which the design should provide additional volume of appropriate fabrics or structure, as well as creating digital avatars or 3D models of body silhouettes on which to simulate interaction with textile materials and clothing structures.

5. CONCLUSION

It has been proven that the use of radius-vector functions provides a sufficiently reliable tool for describing morphological changes in the silhouette of the pregnant woman's body. The derived body silhouette indices (FI1–FI5) describe with sufficient accuracy both global and local changes in body shape during the gestational period.

It has been established that the indices of symmetry, convexity, local curvature, and dynamics of the silhouette of the pregnant woman's body show a sufficiently high sensitivity to changes in the female body with the progress of pregnancy. They correlate significantly with basic anthropometric

parameters such as body mass (BM) and waist circumference (M), which is a suitable basis for creating regression models with prognostic value and statistical reliability.
The results of the available literature have been supplemented by introducing a formalized mathematical apparatus for geometric analysis of the human body silhouette using radius-vector functions. This builds on existing approaches that are based primarily on linear dimensions and do not sufficiently account for the complexity of the transformations of the human body during pregnancy.

The research should be continued with the integration of radius-vector analysis with 3D scanning technologies for more precise determination of changes in the silhouette of the human body during pregnancy and the application of body silhouette indices in algorithms for automated design of adaptive clothing for pregnant women, as well as the development of virtual avatars and simulation models for visualization and testing of interaction with clothing designs.

APPENDIX A

Figure A1 shows 81 silhouettes of women's bodies during the stages of pregnancy. "Mx" indicates the months of pregnancy. A nine-column grid is used in the illustration, labeled M1 to M9, to map out each month of pregnancy. In every column, red-dot silhouettes show how a pregnant woman's body changes as time goes on. At first, from M1 to M3, the changes are barely noticeable. Then, around the middle months (M4 to M6), the belly started to grow. By the last months, M7 to M9, the abdominal expansion is hard to miss. This month-by-month setup makes it easy to follow the gradual transformation and compare how the body shape shifts as pregnancy moves along.

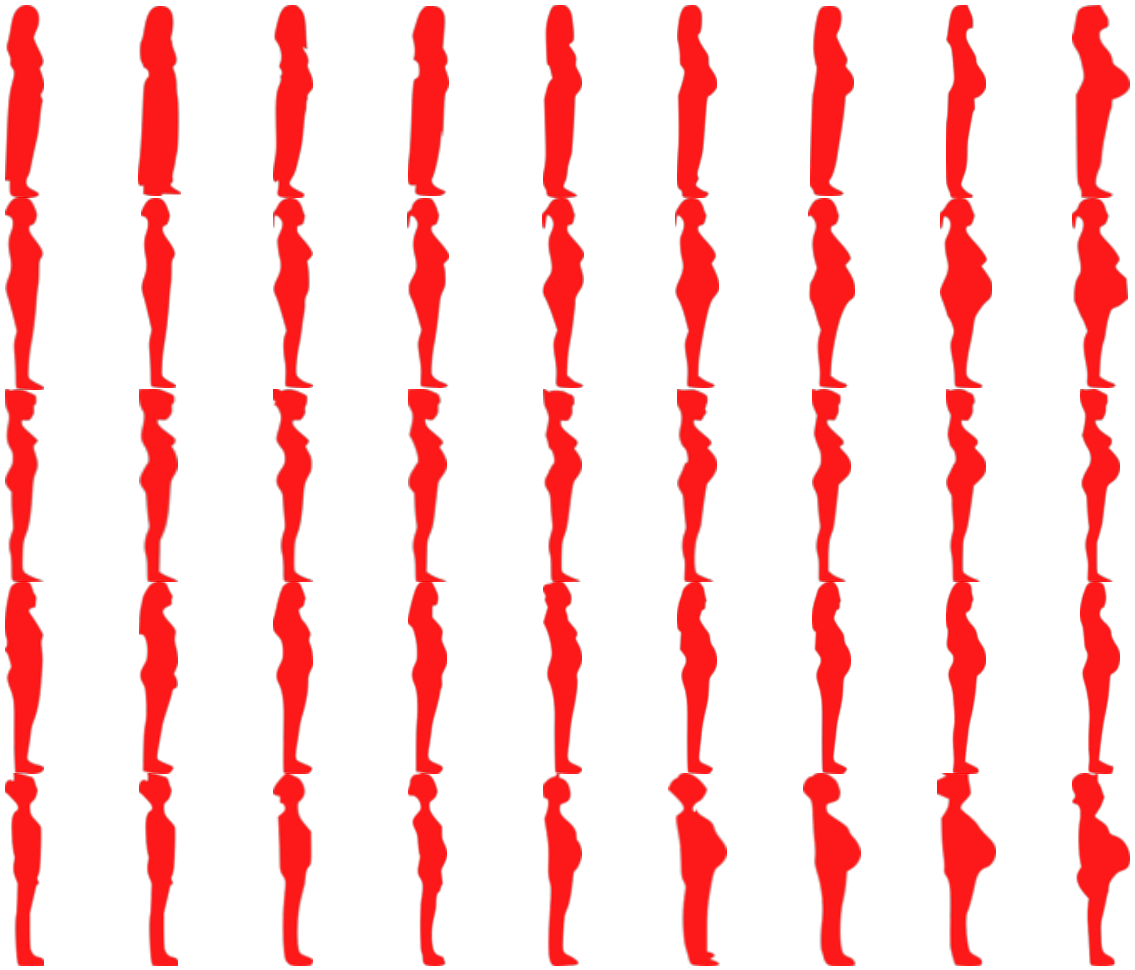

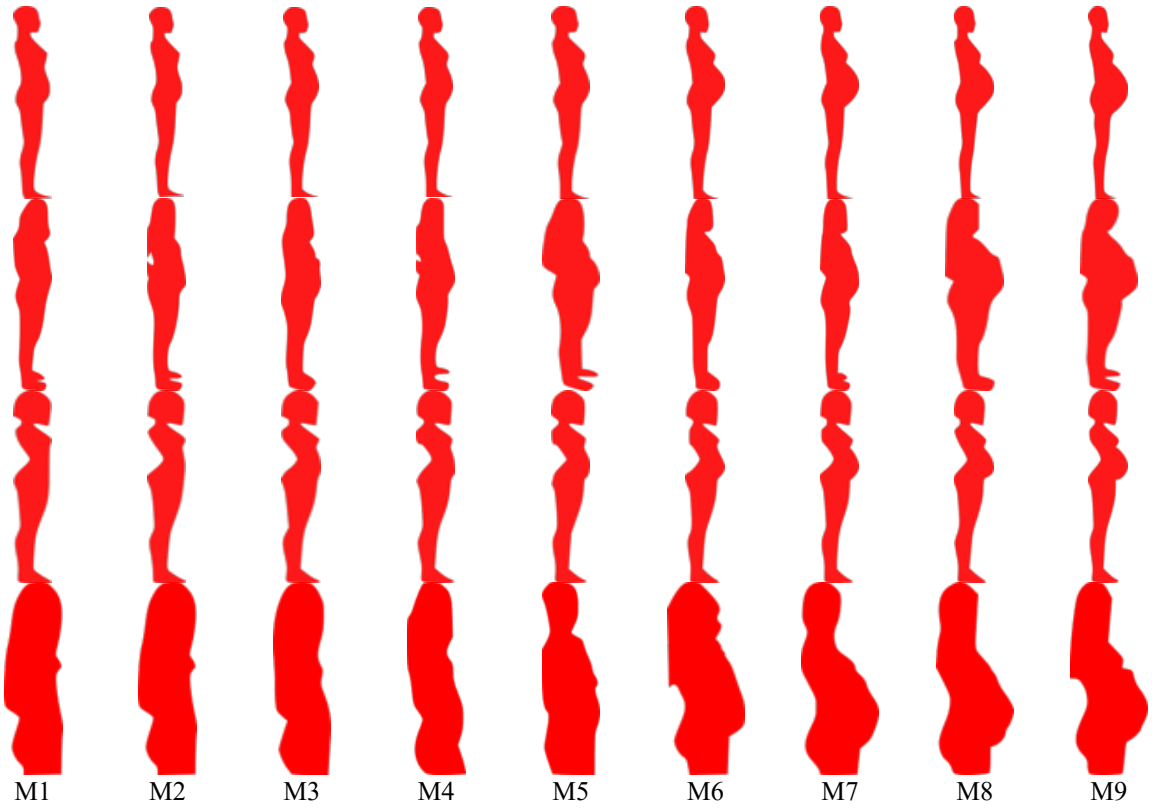

***Fig. A1**: Silhouettes of women's bodies during the stages of pregnancy*

REFERENCES

[1] Centers for Disease Control and Prevention, Anthropometry Procedures Manual. National Health and Nutrition Examination Survey (NHANES III), 1996. [Online]. Available: https://wwwn.cdc.gov/nchs/Data/Nhanes3/Manuals/anthro.pdf

[2] International Organization for Standardization, ISO 8559-1:2017 – Size designation of clothes – Anthropometric definitions and body measurement procedures. Geneva, Switzerland: ISO, 2017.

[3] International Organization for Standardization, ISO 20685-1:2018 – 3-D scanning methodologies for internationally compatible anthropometric databases. Geneva, Switzerland: ISO, 2018.

[4] Fytted, "How accurate are body measurements from photos?" 2025. [Online]. Available: https://www.fytted.com/blog/photo-measurement-accuracy-2025.

[5] O. Koval and M. Koval, "Quantitative comparison of manual and 3D body scanner measurements," in Proc. 3DBODY.TECH Conf., 2020. [Online]. Available: https://proc.3dbody.tech/papers/2020/2035koval.pdf

[6] J. Lee, S. Kim, and H. Park, "Comparison of body scanner and manual anthropometric measurements: A systematic review," Int. J. Environ. Res. Public Health, vol. 18, no. 12, p. 6213, 2021. doi: 10.3390/ijerph18126213.

[7] A. Jaiswal, "Smart motherhood wear: A solution to the problem of maternity wear," Int. J. Home Sci., vol. 8, no. 1, pp. 278–281, 2022.

[8] S. Tripathi, M. Sharma, and P. Sinha, "Innovative clothing design for maternity wear," Int. J. Home Sci., vol. 3, no. 3, pp. 151–154, 2017.

[9] M. Balasubramanian, A. Petrova, and K. Robinette, "Anthropometric dynamics of pregnant women and their implications on apparel sizing," in Proc. Int. Conf. 3D Body Scanning Technologies, Long Beach, CA, USA, Nov. 19–20, 2013, pp. 439–446.

[10] T. J. García Flores and P. M. Pascua Cantarero, "Evaluation of the impact of 3D scanning and photogrammetry methods on anthropometric university practices: A case study," J. Mach. Intell. Data Sci., vol. 5, pp. 82–93, 2024. doi: 10.11159/jmids.2024.010.

[11] M. Rani and N. Dahiya, "Comprehensive study on shape representation methods in image processing: A review," Sādhanā, vol. 48, no. 13, pp. 1–17, 2023. doi: 10.1007/s12046-023-02017-3.

[12] Y. H. Wong, M. A. Rahman, and M. Rizon, "A set of bilateral and radial symmetry shape descriptors for object classification," IET Comput. Vis., vol. 11, no. 4, pp. 303–311, 2017. doi: 10.1049/iet-cvi.2015.0413.

[13] K. Gościewska and D. Frejlichowski, "The analysis of shape features for the purpose of exercise types classification using silhouette sequences," Applied Sciences, vol. 10, no. 19, p. 6728, 2020. doi: 10.3390/app10196728.

[14] L. F. Costa and R. M. Cesar, Jr., Shape Analysis and Classification: Theory and Practice. Boca Raton, FL, USA: CRC Press, 2001.

[15] M. D. Klarqvist, Q. F. Wills, et al., "Prediction of fat depot volumes from silhouette images using deep learning," Commun. Med., vol. 2, p. 74, 2022. doi: 10.1038/s43856-022-00124-y.

[16] H. J. Miller, "A measurement theory for time geography," Geogr. Anal., vol. 33, no. 4, pp. 367–386, 2001. doi: 10.1111/j.1538-4632.2001.tb00456.x.

[17] F. J. A. Poirier and A. D. Wilson, "A visual saliency account of figure–ground perception," Front. Psychol., vol. 6, p. 1685, 2015. doi: 10.3389/fpsyg.2015.01685.

[18] FSRNCA, "Feature selection using neighborhood component analysis for regression," MathWorks, 2025. [Online]. Available: https://www.mathworks.com/help/stats/fsrnca.html. Accessed: Jul. 18, 2025.

[19] W. Wei, D. Wang, and J. Liang, "Accelerating ReliefF using information granulation," Int. J. Mach. Learn. Cybern., vol. 13, pp. 29–38, 2022.

[20] SFCPP, "Select subset of features with comparative predictive power," MathWorks, 2025. [Online]. Available: https://www.mathworks.com/help/stats/feature-selection.html. Accessed: Jul. 26, 2025.

[21] A. Farrell, G. Wan, S. Rush, J. Martin, J. Belant, A. Butler, and D. Godwin, "Machine learning of large-scale spatial distributions of wild turkeys with high-dimensional environmental data," Ecology and Evolution, pp. 1–12, 2019.

[22] TK-Yambol Project, Research into the change in some dimensional features of the female body during pregnancy, necessary for the design of maternity clothing (in Bulgarian), 2001.

[23] Ts. Georgieva, A. Mihaylova, and P. Daskalov, "Research of the possibilities for determination of some basic soil properties using image processing," in Proc. 7th Int. Conf. Energy Efficiency and Agricultural Engineering (EE&AE), 2020, pp. 1–4.

[24] E. B. Salzer, J. F. F. Meireles, A. F. Â. Toledo, M. R. de Siqueira, M. E. C. Ferreira, and C. M. Neves, "Body image assessment tools in pregnant women: A systematic review," Int. J. Environ. Res. Public Health, vol. 20, no. 3, p. 2258, 2023. doi: 10.3390/ijerph20032258.

[25] C. Bao, Y. Miao, J. Chen, and X. Zhang, "Developing a generalized regression forecasting network for the prediction of human body dimensions," Applied Sciences, vol. 13, no. 18, p. 10317, 2023. doi: 10.3390/app131810317.

[26] J. Bicevskis, Z. Bicevska, E. Diebelis, and L. Purina, "Quality control of body measurement data using linear regression methods," in Proc. 19th Conf. Computer Science and Intelligence Systems (FedCSIS), vol. 39, pp. 289–300, 2024. doi: 10.15439/2024F6463.

[27] V. Choutas, L. Müller, C.-H. P. Huang, S. Tang, D. Tzionas, and M. J. Black, "Accurate 3D body shape regression using metric and semantic attributes," in Proc. IEEE/CVF Conf. Computer Vision and Pattern Recognition (CVPR), 2022. doi: 10.48550/arXiv.2206.07036.